Chiral recognition of (18-crown-6)-tetracarboxylic acid as a chiral selector determined by NMR spectroscopy

Eunjung Bang,[a,b] Jin-Won Jung,[c] Wonjae Lee,*[d] Dai Woon Lee *[a] and Weontae Lee *[c]

[a] *Department of Chemistry, Yonsei University, Seoul, 120-749, Korea*
[b] *Korea Basic Science Institute, Seoul Branch, Seoul, 136-701, Korea*
[c] *Department of Biochemistry, Yonsei University, Seoul, 120-749, Korea*
[d] *College of Pharmacy, Chosun University, Kwangju, 501-709, Korea*

Received (in Cambridge, UK) 5th March 2001, Accepted 15th June 2001
First published as an Advance Article on the web 2nd August 2001

It is shown that the chiral selector (+)-(18-crown-6)-2,3,11,12-tetracarboxylic acid (18-C-6-TA) employed for resolution of α-amino acids in capillary electrophoresis and in chiral HPLC can be used for resolution of α-amino acids and ester derivatives in NMR experiments. In a quest for the origin of chiral recognition of α-amino acids in the presence of 18-C-6-TA as a chiral selector, these interactions responsible for the differential affinities shown toward enantiomers are investigated by NMR spectroscopy. Chemical-shift differences of the corresponding ^{1}H and ^{13}C resonances of D- and L-phenylglycine (PG) or phenylglycine methyl ester (PG-ME) show that most chemical shifts in the presence of 18-C-6-TA moved in the same direction (*i.e.*, upfield or downfield) as compared with those of the free state. Significant reduction of the T_1-values is observed for the host–guest complex molecules, indicating that the mobility of the isomers is significantly reduced due to tight binding with 18-C-6-TA. NMR line broadening of the analyte upon complexation further supports this finding. The observed intermolecular NOEs of the α-proton and *ortho* phenyl protons of PG or PG-ME in the presence of 18-C-6-TA are used for generating structures for 18-C-6-TA/enantiomer complexes. Molecular dynamics calculations based on NOEs illustrate the essential features of the chiral recognition mechanism: 1) three $^{+}NH\cdots O$ hydrogen bonds in a tripod arrangement between polyether oxygens of 18-C-6-TA and the ammonium moiety of the enantiomer; 2) a hydrophobic interaction between the polyether ring of 18-C-6-TA and the phenyl moiety of the enantiomer; 3) hydrogen bonding between the carboxylic acid of 18-C-6-TA and the carbonyl oxygen of the D-enantiomer.

Introduction

Chiral recognition, the process in which a particular chiral molecule or molecular group (host) specifically recognizes a stereoisomer (guest), is one of the essential reaction processes occurring in living systems. Therefore, the chemical or biological activity of a compound often depends upon its stereochemistry in living organisms.[1] This gives rise to consequences for chemical substances used as pharmaceuticals, agrochemicals and flavors. A number of synthetic model compounds have been designed and synthesized as chiral host molecules to help chemists understand the basis of the mechanism of host–guest complexations and their chiral recognitions. Their complexation and chiral recognition mechanisms are mainly due to noncovalent interactions between host and guest chiral molecules which are found not only in synthetic supramolecular complexes, but also in biomimetic and biological molecules.[2] Therefore, detailed investigation of chiral recognition phenomena through elucidation of noncovalent interactions has been constantly required for the basis of new approaches in the fields of pharmaceutical chemistry and biochemistry.[2,3]

Crown ethers, a class of synthetic host molecules, have aroused considerable interest because they bind not only alkali cations but also protonated amines with high selectivity and affinity.[4] Many studies using crown ethers as chiral selectors have been effectively accomplished for resolution of racemic α-amino acids and primary amines by liquid–liquid extraction and high-performance liquid chromatography.[4–6] Among several chiral crown ether derivatives, (+)-(18-crown-6)-2,3,11,12-tetracarboxylic acid **1** (18-C-6-TA) prepared from L-tartaric acid by Lehn and his co-workers[7] has been employed in capillary electrophoresis to resolve the enantiomers of α-amino acids and primary amines. Fig. 1[8] We recently reported the synthesis and evaluation of a new chiral stationary phase (CSP) prepared by bonding 18-C-6-TA to aminopropyl silica gel.[9] This CSP was successfully utilized in resolving not only various α-amino acids, but also their ester and amide derivatives.[9b] It was also found to be capable of separating the enantiomers of primary amines including amino alcohols and quinolone antibacterials.[9a,d] More recently, we developed a dynamic CSP prepared by hydrophobically bonding the *N*-dodecyl diamide of 18-C-6-TA to octadecyl silica gel. It was also successfully employed in resolving various racemic compounds containing a primary amino group as well as α-amino

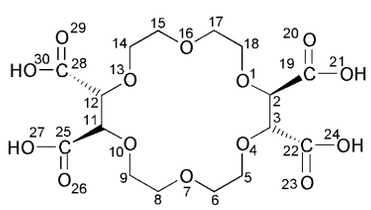

1 (18-C-6-TA)

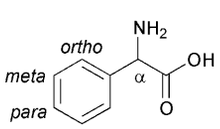

2 (PG)

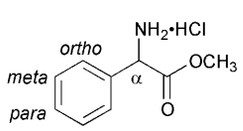

3 (PG-ME)

Fig. 1 Chemical structures of 18-C-6-TA **1**, PG **2** and PG-ME **3**.

acids.[10] All 27 natural and unnatural racemic α-amino acids which were analytes were resolved on a CSP prepared by covalently bonding 18-C-6-TA to aminopropyl silica gel with reasonable separation factors ($\alpha = 1.10$–2.30), except for proline, lacking a primary amino group.[9b] Except for threonine analyte, consistent elution orders of the examined α-amino acids were observed, showing that the D-enantiomers interact more strongly with the chiral selector than do L-enantiomers.[9b,10]

Our interests focus on elucidation of the interactions responsible for the differential affinities shown toward enantiomers by the chiral selector of 18-C-6-TA. The solution NMR data including intra- and intermolecular nuclear Overhauser effects (NOE) have been shown to be especially powerful in providing information regarding conformational preferences of chiral selector–selectand (host–guest) complexes present in the solution state.[11] Therefore, in this study, we performed detailed NMR studies for each enantiomer of phenylglycine **2** (PG) and phenylglycine methyl ester **3** (PG-ME) with 18-C-6-TA to investigate the chiral-recognition mechanism of the diastereomeric complexes in the solution state.

Results and discussion

Correlation between chiral recognition and chemical shifts

The chiral selector 18-C-6-TA has been particularly useful for the enantioseparation of α-amino acids by capillary electrophoresis.[8] Also, 18-C-6-TA-derived CSPs which were recently developed in HPLC have been found to be very effective in resolving not only amino acids, but also various analytes containing a primary amino group, such as quinolone antibacterials.[9,10,12] Since 18-C-6-TA has been successfully employed as a chiral selector in resolving various amino acids in capillary electrophoresis as well as in HPLC, it was expected that it could be useful for enantiodiscrimination of these kinds of analytes in solution NMR. Although racemic PG was not resolved in spite of its long migration time (*ca*. 60 min) by capillary electrophoresis with the use of 18-C-6-TA, CSPs derived from 18-C-6-TA by HPLC have been found to be very effective in resolving not only racemic PG but also PG-ME.[9b,10] Therefore, we performed NMR studies for chiral discrimination of PG and PG-ME.

When an equimolecular amount of 18-C-6-TA was added to racemic PG or PG-ME, both α-proton and *ortho* phenyl protons (or methyl protons) of PG or PG-ME were split into two singlet peaks or two sets, indicating that 18-C-6-TA discriminates successfully both PG and PG-ME in NMR as well as in HPLC environments. ^{1}H NMR spectra of PG and PG-ME in the presence of 18-C-6-TA at 30 °C are shown in Fig. 2 and Fig. 3. The resonance assignments of analytes were completed by the combined use of 2D double-quantum-filtered correlation spectroscopy (DQF-COSY)[13] and heteronuclear multiquantum correlation (HMQC)[14] spectra. The HMQC spectrum of *rac*-PG in the presence of 18-C-6-TA is shown in Fig. 4. Two sets of sixteen methylene protons of 18-C-6-TA were separated into three sets in the presence of PG analyte, and were identified as four *cis* protons relative to COOH on OCH_2 (5 down, 9 up, 14 down, 18 up), four *trans* protons to COOH on OCH_2 (5 up, 9 down, 14 up, 18 down) and eight OCH_2 protons (up and down of C-6, C-8, C-15, C-17) in Fig. 2.

Chemical-shift assignments of both ^{1}H and ^{13}C for PG and PG-ME are summarized in Tables 1 and 2. Chemical-shift differences of the corresponding ^{1}H and ^{13}C resonances of D- and L-forms obtained by subtracting the L-isomer- from D-isomer-values showed that most chemical shifts in the presence of 18-C-6-TA were moved in the same direction compared with their chemical shifts of the free state. This implies that the binding pattern (or complex geometry) is very similar in each case; however, the detailed binding mechanism and binding affinity between two isomers are different. In general, the proton chemical shift-changes of D-isomers upon complexation are greater than those of L-isomers. In particular, the Chemical-shift change of the α-proton is greater than that of any other proton. For example, the fairly large Chemical-shift differences of the α-proton for the equimolecular solution of 18-C-6-TA and PG or PG-ME were observed as $\Delta\Delta\delta = 0.21$ ppm for PG, 0.23 for PG-ME and, therefore, the α-protons of the D-enantiomers were shifted more downfield than were those of the L-enantiomers. For ^{13}C resonances, the largest Chemical-shift differences of the α-carbons were also observed as $\Delta\Delta\delta = -0.58$ for PG and -0.38 for PG-ME, respectively. It can be explained that since both α-proton and α-carbon of the analyte are near to the carboxylic acid of the host molecule as well as the ammonium cation of the analyte, they are significantly influenced by the chiral moiety of 18-C-6-TA and intermolecular hydrogen bondings of the ammonium ion. On the other hand, the ^{13}C Chemical-shift differences of the carbonyl carbon of the analyte were observed as $\Delta\Delta\delta = 0.11$ for PG, 0.16 for PG-ME, respectively, showing that the carbonyl carbon resonances of the D-enantiomers were shifted more downfield than were those of the L-enantiomers.

In Fig. 2 and Fig. 3, it was observed that the line broadening of α-proton of D-PG or PG-ME was greater than that of L-PG or PG-ME in the presence of 18-C-6-TA. This implies that the mobility of the D-enantiomer is lower than that of the L-enantiomer in the presence of 18-C-6-TA. Therefore, we expect that the D-enantiomers interact more strongly with the chiral selector than do L-enantiomers. These observations are consistent with our chromatographic data reported previously, showing that the D-enantiomers are preferentially retained on CSPs derived from 18-C-6-TA.[9b,10]

Spin–lattice relaxation-time measurements

Since spin–lattice relaxation time (T_1) is sensitive to molecular motions, it is important to know the different mobilities of two enantiomers through an examination of their relaxation properties in the presence of a chiral selector. All protons of enantiomers upon complexation with 18-C-6-TA **1** demonstrated shorter T_1 relaxation times than those of the free forms (Table 3). In the presence of 18-C-6-TA, the T_1-values for the α-proton and *ortho* phenyl proton of D-PG D-**2** were measured as 1.87 s and 1.82 s, respectively, whereas those for L-PG L-**2** complexed with 18-C-6-TA were 2.22 s and 2.07 s, which were much shorter than those of free PG (4.72 s and 4.22 s). In particular, significant reduction of the T_1-values was observed for the α-proton of PG, **2** indicative of restrictive mobility in the presence of 18-C-6-TA. For the α-proton of PG-ME **3**, the T_1-values were 1.49 s for the D-enantiomer and 1.52 s for the L-enantiomer in the presence of host molecule 18-C-6-TA, and 5.19 s for the free ester, respectively. All these results indicate that the mobility of the complex was much more reduced through 18-C-6-TA binding, which was supported by the NMR line broadening of the analyte upon complexation.

Binding-constant measurements

The continuous-variation method (Job plot)[15] changing the molar fraction from 0.2 to 0.8 was used to determine the stoichiometry, while the total concentrations of 18-C-6-TA **1** and PG **2** or PG-ME **3** enantiomer were kept constant at 10 mM. Fig. 5 shows symmetrical bell-curves for both PG and PG-ME, indicative of the 1 : 1 complexation between chiral selector and selectand. ^{1}H NMR measurements of the α-proton resonance were carried out under the conditions of constant concentration of PG or PG-ME with a varying concentration of 18-C-6-TA. The binding constants K_a for the 1 : 1 complex between 18-C-6-TA and enantiomers were determined by using Scott's modification[16] of the Benesi–Hildebrand equation.[17] Thus the titration data were analyzed using equations (1) and (2):

Table 1 ^{1}H and ^{13}C chemical shifts (ppm) of *rac*-PG **2** in the absence and presence of 18-C-6-TA **1** at 30 °C in methanol-d_4 with 10 mM H_2SO_4

^{1}H NMR	Free[a]	**1**–(L)-**2**[b]	$\Delta\delta$(L)	**1**–(D)-**2**[b]	$\Delta\delta$ (D)	$\Delta\Delta\delta$ (D-L)[c]
α-Proton	5.06	5.26	0.20	5.47	0.41	0.21
ortho	7.49	7.57	0.08	7.64	0.15	0.07
meta/*para*[d]	7.49/7.49	7.45/7.45	N.D.	7.45/7.45	N.D.	N.D.
^{13}C NMR	Free[a]	**1**–(L)-**2**[b]	$\Delta\delta$ (L)	**1**–(D)-**2**[b]	$\Delta\delta$ (D)	$\Delta\Delta\delta$ (D-L)[c]
α-Carbon	57.76	58.03	0.27	57.45	−0.31	−0.58
ortho	129.18	129.74	0.56	129.87	0.69	0.13
meta	130.58	130.30	−0.28	130.05	−0.53	−0.25
para	131.16	131.02	−0.14	130.93	−0.23	−0.09
Quaternary	133.92[e]	134.04	0.12	134.18	0.26	0.14
CO	170.74	170.95	0.21	171.06	0.32	0.11

[a] [*rac*-**2**] = 2 mM. [b] The chemical shifts were based on the spectrum of *rac*-**2** (2 mM) in the presence of **1** (2.2 mM). [c] Obtained by subtracting the **1**–(L)-**2** value from the **1**–(D)-**2** one. [d] Not assigned because of resonance overlap. [e] Measured by [*rac*-**2**] = 20 mM. N.D. = Not determined.

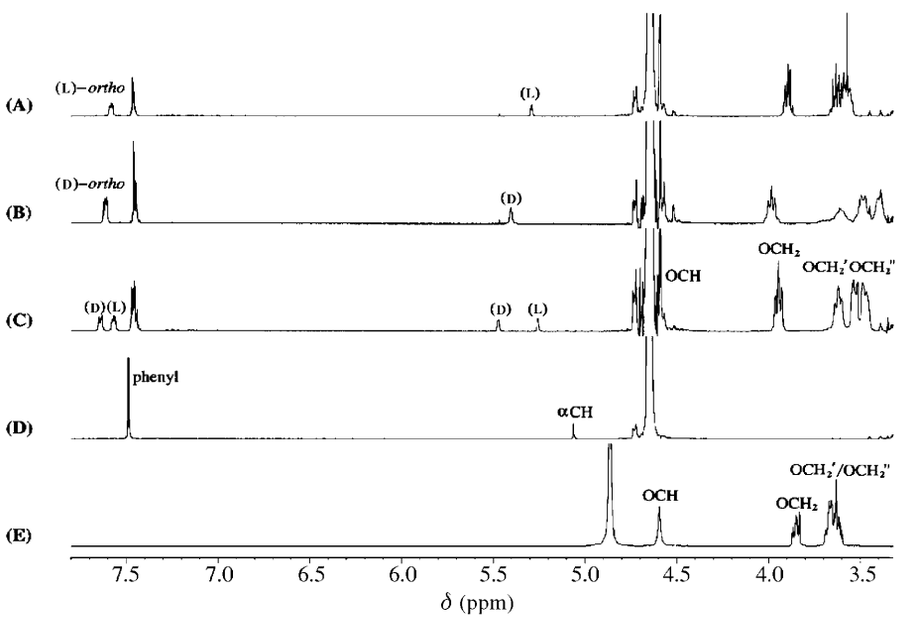

Fig. 2 ^{1}H NMR spectra of PG and PG/18-C-6-TA complex with equimolar mixtures (2 mM each); (A) L-PG with 18-C-6-TA, (B) D-PG with 18-C-6-TA, (C) *rac*-PG with 18-C-6-TA, (D) *rac*-PG, (E) free 18-C-6-TA.

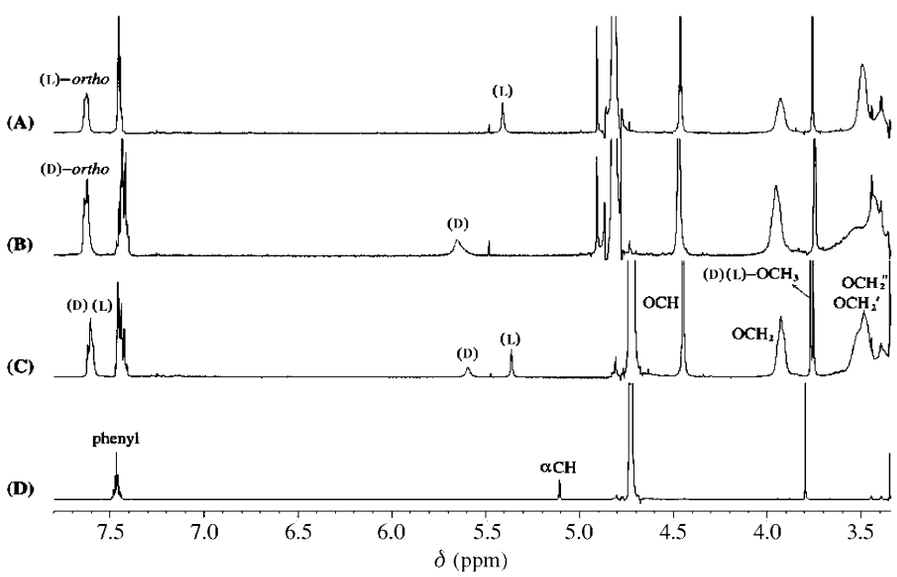

Fig. 3 ^{1}H NMR spectra of PG-ME and PG-ME/18-C-6-TA complex with equimolar mixtures (2 mM each); (A) L-PG-ME with 18-C-6-TA, (B) D-PG-ME with 18-C-6-TA, (C) *rac*-PG-ME with 18-C-6-TA, (D) *rac*-PG-ME.

Table 2 ^{1}H and ^{13}C chemical shifts (ppm) of *rac*-PG-ME **3** in the absence and presence of 18-C-6-TA **1** at 30 °C in methanol-d_4

^{1}H NMR	Free[a]	**1**–(L)-**3**[b]	$\Delta\delta$ (L)	**1**–(D)-**3**[b]	$\Delta\delta$ (D)	$\Delta\Delta\delta$ (D-L)[c]
α-Proton	5.11	5.36	0.25	5.59	0.48	0.23
OCH_3	3.80	3.77	−0.03	3.76	−0.04	−0.01
ortho[d]	7.46	7.60/7.60	N.D.	7.60/7.60	N.D.	N.D.
meta/*para*[d]	7.46/7.46	7.45/7.45	N.D.	7.45/7.45	N.D.	N.D.
^{13}C NMR	Free[a]	**1**–(L)-**3**[b]	$\Delta\delta$ (L)	**1**–(D)-**3**[b]	$\Delta\delta$ (D)	$\Delta\Delta\delta$ (D-L)[c]
α-Carbon	57.96	58.18	0.22	57.80	−0.16	−0.38
OCH_3	53.95	53.87	−0.08	53.80	−0.15	−0.07
ortho	129.08	129.54	0.46	129.85	0.77	0.31
meta	130.65	130.48	−0.17	130.25	−0.40	−0.23
para	131.18	131.17	−0.01	131.13	−0.05	−0.04
Quaternary	134.11	133.54	−0.57	133.58	−0.53	0.04
CO	170.16[e]	170.23	0.07	170.39	0.23	0.16

[a] [*rac*-**3**] = 2 mM. [b] The chemical shifts were based on the spectrum of *rac*-**3** (2 mM) in the presence of **1** (2.2 mM). [c] Obtained by subtracting the **1**–(L)-**3** value from the **1**–(D)-**3** ones. [d] Not assigned because of resonance overlap. [e] Measured by [*rac*-**3**] = 15 mM. N.D. = Not determined.

Table 3 T_1-Values (s) for α-proton and *ortho* phenyl proton of *rac*-PG and *rac*-PG-ME with 18-C-6-TA at 27 °C[a]

	Free-**2**[b]	**1**–(L)-**2**	**1**–(D)-**2**	Free-**3**[c]	**1**–(L)-**3**	**1**–(D)-**3**
α-Proton	4.72	2.22	1.87	5.19	1.52	1.49
ortho	4.22	2.07	1.82	5.37	1.55	1.56

[a] T_1-Values represent the average of six or seven independent experiments, and the deviation was less than 2%. [b] [*rac*-**2**] = 20 mM. [c] [*rac*-**3**] = 15 mM.

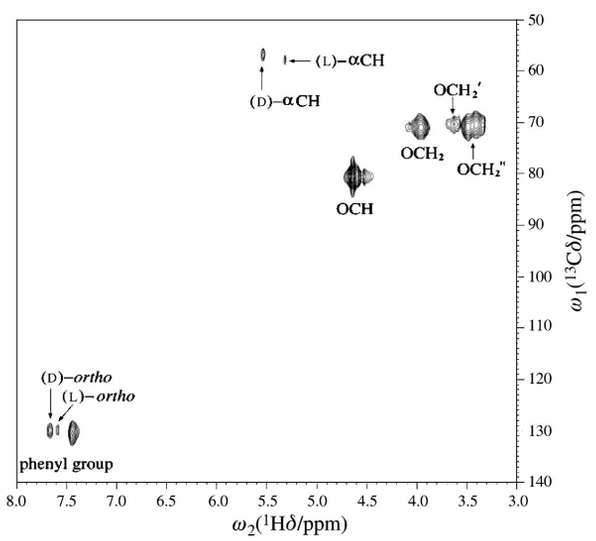

Fig. 4 HMQC spectrum of *rac*-PG dissolved in methanol-d_4 and 10 mM H_2SO_4 in the presence of 18-C-6-TA.

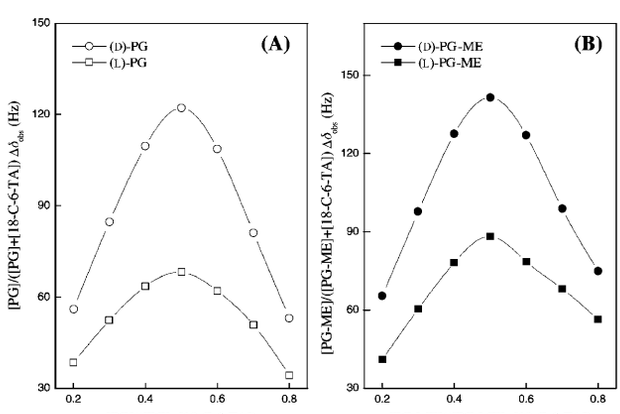

Fig. 5 Job plots for PG and PG-ME enantiomers and 18-C-6-TA; (A) PG, (B) PG-ME.

$$\frac{[\text{18-C-6-TA}]_t}{\Delta\delta_{obs}} = \frac{[\text{18-C-6-TA}]_t}{\Delta\delta_c} + \frac{1}{K_a\Delta\delta_c} \quad (1)$$

$$K_a = \frac{1}{[\text{18-C-6-TA}]_t} \times \frac{\Delta\delta_{obs}}{(\Delta\delta_c - \Delta\delta_{obs})} \quad (2)$$

where $[\text{18-C-6-TA}]_t$ is the molar concentration of the chiral selector, δ_{obs} is the observed Chemical-shift difference of the α-proton of PG **2** or PG-ME **3** for a given $[\text{18-C-6-TA}]_t$ concentration and $\Delta\delta_C$ is the Chemical-shift difference between complex and free analyte under saturation conditions. The concentration of the analyte was kept at 1 mM, while that of 18-C-6-TA was changed from 1 to 5 mM. The addition of 18-C-6-TA **1** to PG **2** or PG-ME **3** enantiomer induced considerable Chemical-shift changes of both α-proton and *ortho* phenyl protons. As shown in Fig. 6, showing Scott plots of $[\text{18-C-6-TA}]_t/\Delta\delta_{obs}$ against $[\text{18-C-6-TA}]_t$, the ratio between $[\text{18-C-6-TA}]_t$ and $\Delta\delta_{obs}$ was correlated with $[\text{18-C-6-TA}]_t$. The binding constants K_a and the complexation-induced chemical shifts $\Delta\delta_C$ were determined from analysis of the slope and intercept (Table 4). The values of $\Delta\delta_C$ of the α-proton on the D-enantiomers were larger than those of the L-enantiomers. Accordingly, the binding constants K_a of the D-enantiomers were larger than those of the L-enantiomers. The separation factors derived from binding-constant measurements were calculated as 4.34 for PG and 1.72 for PG-ME, respectively, which were consistent with those determined by the chiral HPLC method, as shown in Table 4. On a CSP prepared by covalent bonding 18-C-6-TA, the observed separation factors were 2.25 for PG and 2.09 for PG-ME,[9b] respectively. In addition, the separation factors were 4.03 for PG and 2.47 for PG-ME on a CSP prepared by dynamic coating 18-C-6-TA.[10]

Therefore, these enantioselectivities of PG and PG-ME in the presence of 18-C-6-TA in this study agreed with those observed for 18-C-6-TA-derived CSPs in HPLC experiments. The strong complexation of D-enantiomers for these analytes is also consistent with their elution order data in chiral HPLC.[9b,10] Interestingly, it was observed that the enantioselectivity of PG measured in our NMR study is greater than that of PG-ME

Table 4 Binding constants (K_a/mol) and complexation-induced chemical shifts at saturation ($\Delta\delta_C$/ppm) for α-protons of PG and PG-ME with 18-C-6-TA

	K_a(D)	K_a(L)	$\Delta\delta_C$(D)	$\Delta\delta_C$(L)	$\alpha[K_a(D)/K_a(L)]$	α(D/L)[a]	α(D/L)[b]
PG	1034	238	0.57	0.55	4.34	2.25	4.03
PG-ME	1992	1159	0.66	0.42	1.72	2.09	2.47

[a] Separation factors in CSP[9b] prepared by covalent bonding of 18-C-6-TA. [b] Separation factors in CSP[10] prepared by dynamic coating of 18-C-6-TA.

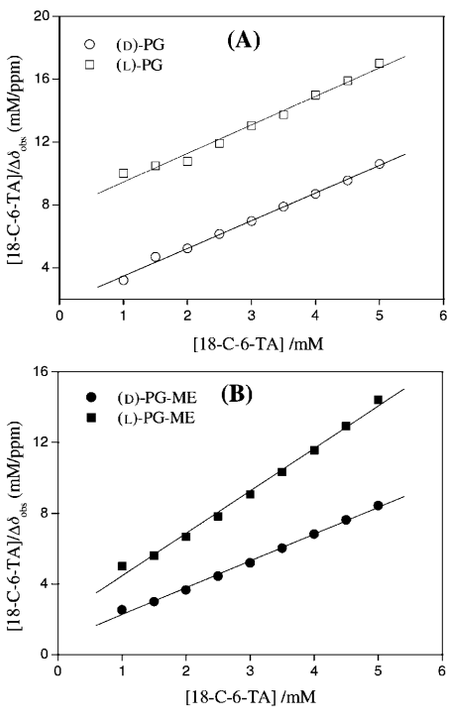

Fig. 6 Scott plots for PG and PG-ME enantiomers (1 mM) and 18-C-6-TA solution (1–5 mM); (A) PG, (B) PG-ME.

(Table 4). The same trend has been observed for CSPs derived from 18-C-6-TA in HPLC.[9b,10]

Compared with the enantioselectivities of PG and PG-ME obtained from NMR titration, the results for a CSP prepared by dynamic coating of 18-C-6-TA are likely to be more suitable than those for a CSP prepared by covalent bonding of 18-C-6-TA. Presumably, the environment of the chiral complexation of PG (or PG-ME) with 18-C-6-TA under NMR conditions might be considered to be similar to that of a dynamic 18-C-6-TA-coated CSP because this CSP would be relatively flexible in aqueous solution. It is interesting that each binding constant of the PG-ME enantiomers was larger than that of the corresponding PG enantiomer in NMR data. Similarly, it has been observed that the retention data of PG-ME are greater than those of PG on the dynamically coated CSP in HPLC, while they have similar values for the covalently bonded CSP.[9b,10]

Intermolecular NOEs between 18-C-6-TA and enantiomers

A number of intramolecular nuclear Overhauser effects (NOEs) for 18-C-6-TA and enantiomers were observed. In addition, intermolecular NOEs between each enantiomer and the chiral selector were observed, as shown in nuclear Overhauser effect spectroscopy (NOESY)[18] spectra of *rac*-PG in the presence of 18-C-6-TA (Fig. 7). Interestingly, some differences in intermolecular NOEs were observed between the two enantiomers (Table 5). For example, *ortho* phenyl protons of PG have NOE contacts with both OCH_2 and OCH_2' of 18-C-6-TA, while the α-proton of L-PG did not show any NOE with OCH_2 of 18-C-6-TA. These NOE data explain how D-PG would have not only a different conformation but also a different binding mode with 18-C-6-TA. NOE differences were also observed for PG-ME, showing that the α-proton of D-PG-ME did not show any NOE with OCH_2' of 18-C-6-TA (Table 5).

Table 5 Intermolecular NOEs of *rac*-PG and *rac*-PG-ME with 18-C-6-TA with intensities in parentheses

18-C-6-TA	PG	PG-ME
OCH_2	D-*ortho* (S[a])	D/L[d]-*ortho* (M[b])
	L-*ortho* (S)	D-α-proton (S)
	D-α-proton (S)	L-α-proton (S)
	L-α-proton (S)	
OCH_2'	D-*ortho* (W[c])	D/L[d]-*ortho* (M)
	L-*ortho* (W)	L-α-proton (W)
	D-α-proton (W)	
OCH_2''	D-*ortho* (W)	D/L[d]-*ortho* (M)
	L-*ortho* (M)	D-α-proton (W)
	D-α-proton (M)	L-α-proton (W)
	L-α-proton (W)	

[a] Strong. [b] Medium. [c] Weak. [d] We could not distinguish between the D-isomer and L-isomer because of resonance overlap. Concentrations were 20 mM for *rac*-PG and 15 mM for *rac*-PG-ME.

Structure and chiral recognition

As mentioned before, both NMR and HPLC data[9b,10] demonstrated that the D-isomers of PG or PG-ME bind with 18-C-6-TA more strongly than do the L-isomers. Fig. 8 and Fig. 9 show the structures of the 18-C-6-TA/PG enantiomer complexes generated using NOE constraints. The lowest-energy structures of 18-C-6-TA/PG complexes illustrate how the polyether ring of 18-C-6-TA forms a cavity to make a stable complex with the guest molecule of PG. It shows that the polyether ring of 18-C-6-TA forms a bowl shape by intramolecular hydrogen bonding (O30–H···O23, 1.55–1.57 Å). Therefore, the upper face of the polyether ring of 18-C-6-TA is opened to allow intermolecular hydrogen bonding with the ammonium moiety of a PG enantiomer, while its bottom surface is blocked by the intramolecular hydrogen bonding of two carboxylic groups on 18-C-6-TA.

During the complexation, three hydrogen bonds (1.90–2.24 Å) between the ammonium ion of the L- or D-isomer of PG and three oxygen atoms (O4, O10, O16) of 18-C-6-TA were formed. The modelling structure of 18-C-6-TA/D-PG complex clearly shows it possesses the optimum distances and angles to stabilize this hydrogen-bonding network, compared with those of 18-C-6-TA/L-PG. Additional hydrophobic interactions between the polyether ring of 18-C-6-TA and the phenyl group of PG enantiomer are clearly observed, although the spatial orientation of the phenyl group on each enantiomer relative to 18-C-6-TA is considerably different. As shown in Fig. 8, interestingly, hydrogen bonding between the carbonyl-oxygen of D-PG and the COOH of 18-C-6-TA was observed, whereas such a hydrogen bonding interaction was not found in the 18-C-6-TA/L-PG complex (Fig. 9). The interatomic distance between the carboxylic acid of 18-C-6-TA and the carbonyl oxygen (O27–H···O) of D-PG is 1.67 Å. This hydrogen-bonding interaction in 18-C-6-TA/D-PG complex can be considered to be crucial for effective chiral discrimination. This intermolecular hydrogen-

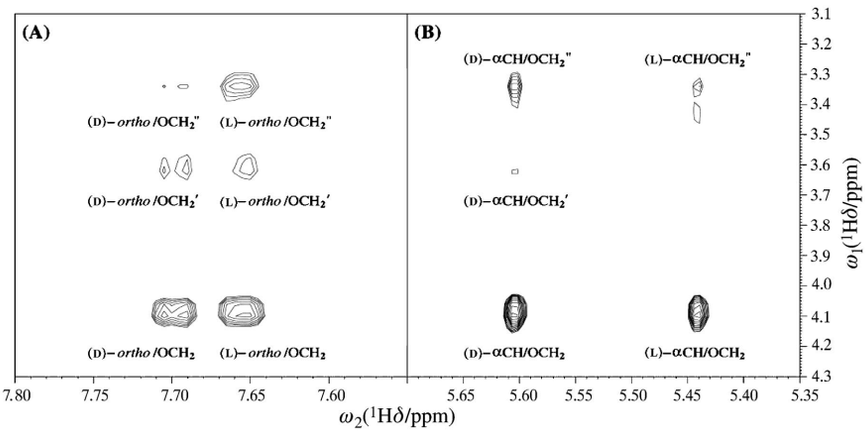

Fig. 7 Expanded NOESY spectra of (A) phenyl region of *rac*-PG, (B) α-proton region of *rac*-PG in the presence of 18-C-6-TA at 30 °C. The concentration was kept at 20 mM, and NOE mixing time was 400 ms.

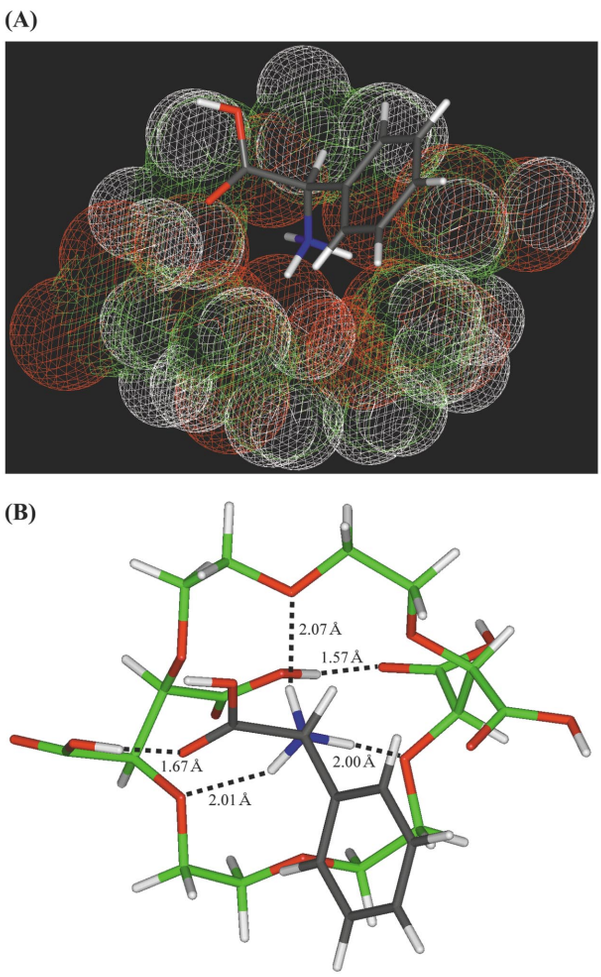

Fig. 8 Structure of 18-C-6-TA/D-PG complex generated from NOE data and molecular dynamics calculations. The structure of the 18-C-6-TA/D-PG complex is shown using both van der Waals radii for 18-C-6-TA and stick representation of D-PG (A). Inter- and intramolecular hydrogen bondings of the 18-C-6-TA/D-PG complex are displayed by dotted lines (B).

bonding interaction rationalizes the fact that the carbonyl ^{13}C resonance of D-PG was observed at a more downfield shift than that of L-PG in NMR experiments (Table 1). In Fig. 8 and Fig. 9, the relative orientations of the α-proton of D-PG and L-PG are nearly identical. On the other hand those of the phenyl moiety and the carboxylic acid group are switched relative to each other, as suggested by the intermolecular NOEs of the α-proton and *ortho* phenyl protons (Table 5 and Fig. 7). Therefore, we can conclude that the D-isomer would form a more favorable complex with chiral selector 18-C-6-TA than would the L-isomer. Consequently, molecular dynamics calculations based on NOE data in NMR studies showed that the ammonium moiety held inside the cavity is bound by three $^{+}NH\cdots O$ hydrogen bonds in a tripod arrangement, hence chiral discrimination is achieved by secondary lateral interactions between the substituents (the carboxylic acid moiety and the polyether ring) on 18-C-6-TA and the analyte (the carbonyl group and the phenyl moiety), which are hydrogen-bonding and hydrophobic interactions, respectively.[8a,19] In particular we suggest that the hydrogen bonding between the carboxylic acid of 18-C-6-TA and the carbonyl oxygen of the D-enantiomer of PG affects chiral discrimination most significantly for the analytes employed.

Therefore, we propose that our findings of a chiral-recognition mechanism between each enantiomer of PG and 18-C-6-TA as a chiral selector could be an essential criterion as well as providing valuable information for new applications of chiral resolution of related compounds and the development of improved chiral selectors.

Experimental

Reagents

D-, L-, *rac*-Phenylglycine **2** and D-, L-phenylglycine methyl ester·HCl **3** were purchased from Aldrich (Milwaukee, WI). Methanol-d_4 and tetramethylsilane (TMS) were from Aldrich (Milwaukee, WI), and 18-C-6-TA **1** was from Fluka (Switzerland). All reagents used were of reagent grade. All samples were prepared as follows: L-isomer and 18-C-6-TA; D-isomer and 18-C-6-TA; *rac*-analyte and 18-C-6-TA; *rac*-analyte. Methanol-d_4–10 mM H_2SO_4 was used for PG analyte, whereas methanol-d_4 was used for PG-ME analyte. Sample concentrations of both individual components and mixtures were in the range 2–20 mM. The stoichiometry between 18-C-6-TA and enantiomer (or racemic) analyte for all NMR experiments ranged from 1.1 : 1 to 5 : 1.

One-dimensional NMR

A series of one-dimensional ^1H and ^{13}C NMR experiments was performed on a Bruker AMX500 or DRX500 operating at 500.1 and 125.7 MHz for ^1H and ^{13}C nuclei, respectively, in the ^2H lock mode. The spectral widths were 5954.5 Hz for ^1H and 31250.0 Hz for ^{13}C, respectively. ^1H and ^{13}C measurements were performed with digital resolutions of 0.17 and 0.95 Hz, respectively. The relaxation delay was set to 4 s for all one-dimensional experiments except T_1 measurements. The sample temperature ranged from 27 to 30 °C. All chemical shifts were referenced to TMS.

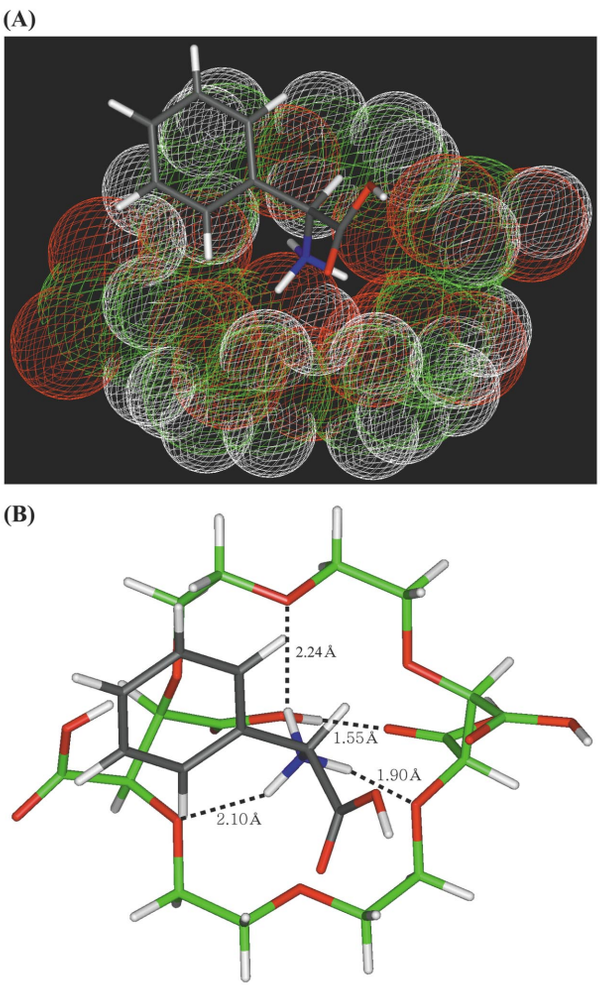

Fig. 9 Structure of 18-C-6-TA/L-PG complex generated from NOE data and molecular dynamics calculations. The structure of the 18-C-6-TA/L-PG complex is shown using van der Waals radii for 18-C-6-TA and stick representation of L-PG (A). Inter- and intramolecular hydrogen bondings of the 18-C-6-TA/L-PG complex are displayed by dotted lines (B).

Spin–lattice relaxation-time measurements

T_1-Values were measured by the inversion recovery method[20] at 27 °C and calculated by a standard program supplied by Bruker Instruments Inc. Fourteen different τ delays varying from 0.0001 to 20 s between 180° and 90° pulses and 30 s relaxation time with 16 scans were used for ^{1}H T_1 measurements. Samples were degassed by sparging with nitrogen gas. T_1-Values represent the average of six or seven independent experiments, and the deviation was less than 2%.

Job plot

The stoichiometry of the complex between 18-C-6-TA and the PG or PG-ME enantiomer was determined by a continuous-variation plot (Job plot).[15] The total concentration of the interacting species in the solution was kept constant at 10 mM and the molar fraction of the chiral selector varied in the range 0.2–0.8. ^{1}H NMR spectra for each sample were taken at 27 °C and the α-proton resonance of PG or PG-ME was also analyzed.

^{1}H NMR titration

The binding constants of the enantiomers of PG and PG-ME with 18-C-6-TA were determined on the basis of Scott's modification of the Benesi–Hildebrand equation.[16,17] In these measurements the concentration of each enantiomer was kept at 1 mM, while the concentration of 18-C-6-TA ranged from 1 to 5 mM. The Chemical-shift changes of the α-proton of PG or PG-ME were used for this plot.

Two-dimensional NMR

2D NMR spectra were recorded in the phase-sensitive mode using time-proportional phase incrementation (TPPI) for quadrature detection in the t_1 domain.[21] NOESY[18] was performed for mixing times of 300–600 ms with and without pulsed filtered gradient (PFG) techniques. NOESY spectra were collected into 2048 data points for 128 or 256 increments with spectral widths of 5000 Hz. Rotating-frame Overhauser effect spectroscopy (ROESY)[22] was performed for mixing times of 200–400 ms. DQF-COSY,[13] HMQC[14] and heteronuclear multiple-bond correlation (HMBC)[23] were performed for resonance assignments of the complex as well as 18-C-6-TA. NMR data were processed on a Silicon Graphics Indigo^2 workstation using the nmrPipe/nmrDraw program (Biosym/Molecular Simulations, Inc.) and XWIN-NMR (Bruker Instruments Inc.) software.

Structure calculations

Starting structures of 18-C-6-TA and PG were constructed using the BUILDER module of INSIGHT II (Molecular Simulations Inc., San Diego, USA) and the structure of 18-C-6-TA was calculated by MM+ force-field-modified MM2 as implemented with Hyperchem 5.0 (Hypercube, Inc., Gainesville, USA) running on a Window NT system. Since the energy of 18-C-6-TA is largely dependent on its ring conformation, an extensive conformational search procedure was performed by Monte Carlo search[24] through restricted ranges from torsion flexing[25] in Chemplus 1.6. The complex structures of both 18-C-6-TA/D-PG and 18-C-6-TA/L-PG were generated using previously determined lowest-energy conformation of 18-C-6-TA and the enantiomers. The structure of 18-C-6-TA was assumed to have C_2 symmetry, implying that only one mode of hydrogen-bonding pattern is available between the ammonium ion of PG and oxygens in the polyether ring of 18-C-6-TA. The complex structures were assembled and optimized by molecular modelling system and molecular dynamics simulation using the INSIGHT II program and DISCOVER 3 module (Molecular Simulations Inc.). We used a distance-dependent relative permittivity implemented in the INSIGHT II program for structural calculations, while the cutoff for nonbonding terms was not set. To obtain the lowest-energy-complex structure, restraint molecular dynamics simulation was performed for 250 ps at 298 K. The upper bound of distance restraint is derived from NOE intensities; 2.5 Å for strong, 3.3 Å for medium, and 5 Å for weak NOE. During the dynamics simulation, conformations were sampled every 100 steps, 0.1 ps. The lowest-energy conformation from MD energy trajectory was regularized by restrained energy-minimization calculations with the BFGS (Broyden–Fletcher–Goldfarb–Shanno) method until the deviation of its energy gradient reached 0.001 kcal mol^{-1}.†

Acknowledgements

This work was supported by the Korean Science and Engineering Foundation (KOSEF) through the Center for Protein Network Research (PNRC) at Yonsei University (Weontae Lee).

† 1 cal = 4.184 J.

References

1 (*a*) R. A. Sheldon, *Chirotechnology: Industrial Synthesis of Optically Active Compounds*, Marcel Dekker, New York, 1993, pp. 39–72; (*b*) H. van der Goot and H. Timmerman, in *Stereoselectivity of Pesticides*, ed. E. J. Ariëns, J. J. S. van Rensen and W. Welling, Elsevier, Amsterdam, 1988, pp. 11–38; (*c*) C. A. White, in *A Practical Approach to Chiral Separations by Liquid Chromatography*, ed. G. Subramanian, VCH, New York, 1994; (*d*) J. Cardwell, *J. Chromatogr. A*, 1995, **694**, 39.

2 H.-J. Schneider, *Angew. Chem., Int. Ed. Engl.*, 1991, **30**, 1417.
3 (*a*) J.-M. Lehn, *Angew. Chem., Int. Ed. Engl.*, 1988, **27**, 89; (*b*) R. M. Kellogg, *Angew. Chem., Int. Ed. Engl.*, 1984, **23**, 782.
4 (*a*) X. X. Zhang, J. S. Bradshaw and R. M. Izatt, *Chem. Rev.*, 1997, **97**, 3313; (*b*) D. J. Cram, *Angew. Chem., Int. Ed. Engl.*, 1988, **27**, 1009; (*c*) E. Weber and F. Vögtle, in *Host Guest Complex Chemistry – Macrocycles*, ed. F. Vögtle and E. Weber, Springer-Verlag, Berlin, 1985, pp. 1–41.
5 A. Shibukawa and T. Nakagawa, in *Chiral Separations by HPLC: Applications to Pharmaceutical Compounds*, ed. A. M. Krstulovic, Wiley, New York, 1989, pp. 476–509.
6 (*a*) T. Shinbo, T. Yamaguchi, K. Nishimura and M. Sugiura, *J. Chromatogr.*, 1987, **405**, 145; (*b*) M. Hilton and D. W. Armstrong, *J. Liq. Chromatogr.*, 1991, **14**, 9; (*c*) T. Shinbo, T. Yamaguchi, H. Yanagishita, D. Kitamoto, K. Sakaki and M. Sugiura, *J. Chromatogr.*, 1992, **625**, 101; (*d*) W. Lee and C. Y. Hong, *J. Chromatogr. A*, 2000, **879**, 113.
7 J.-M. Girodeau, J.-M. Lehn and J.-P. Sauvage, *Angew. Chem., Int. Ed.*, 1975, **14**, 764.
8 (*a*) R. Kuhn, F. Erni, T. Bereuter and J. Hausler, *Anal. Chem.*, 1992, **64**, 2815; (*b*) R. Kuhn, J. Wagner, Y. Walbroehl and T. Bereuter, *Electrophoresis*, 1994, **15**, 828; (*c*) R. Kuhn, D. Riester, B. Fleckenstein and K.-H. Wiesmuller, *J. Chromatogr. A*, 1995, **716**, 371; (*d*) K. Verleysen, J. Vandijck, M. Schelfault and P. Sandra, *J. High Resolut. Chromatogr.*, 1998, **21**, 323; (*e*) K. Verleysen and P. Sandra, *J. Microcolumn Sep.*, 1999, **11**, 37.
9 (*a*) M. H. Hyun, J. S. Jin and W. Lee, *Bull. Korean Chem. Soc.*, 1998, **19**, 819; (*b*) M. H. Hyun, J. S. Jin and W. Lee, *J. Chromatogr. A*, 1998, **822**, 155; (*c*) M. H. Hyun, J. S. Jin, H. J. Koo and W. Lee, *J. Chromatogr. A*, 1999, **837**, 75; (*d*) M. H. Hyun, S. C. Han, J. S. Jin and W. Lee, *Chromatographia*, 2000, **52**, 473.
10 M. H. Hyun, H. J. Koo, J. S. Jin and W. Lee, *J. Liq. Chromatogr. Relat. Technol.*, 2000, **23**, 2669.
11 (*a*) W. H. Pirkle and T. C. Pochapsky, *J. Am. Chem. Soc.*, 1987, **109**, 5975; (*b*) J. M. Coteron, C. Vicent, C. Bosso and S. Penades, *J. Am. Chem. Soc.*, 1993, **115**, 10066; (*c*) E. Yashima, C. Yamamoto and Y. Okamoto, *J. Am. Chem. Soc.*, 1996, **118**, 4036; (*d*) W. H. Pirkle, P. G. Murray, D. J. Rausch and S. T. McKenna, *J. Org. Chem.*, 1996, **61**, 4769.
12 (*a*) Y. Machida, H. Nishi, K. Nakamura, H. Nakai and T. Sato, *J. Chromatogr. A*, 1998, **805**, 85; (*b*) Y. Machida, H. Nishi and K. Nakamura, *J. Chromatogr. A*, 1998, **810**, 33.
13 M. Rance, O. W. Sorensen, G. Bodenhausen, G. Wagner, R. R. Ernst and K. Wuthrich, *Biochem. Biophys. Res. Commun.*, 1983, **117**, 479.
14 A. Bax and S. Subramanian, *J. Magn. Reson.*, 1986, **67**, 565.
15 P. Job, *Ann. Chim. (Paris)*, 1928, **9**, 113.
16 R. L. Scott, *Recl. Trav. Chim. Pays-Bas*, 1956, **75**, 787.
17 H. A. Benesi and J. H. Hildebrand, *J. Am. Chem. Soc.*, 1949, **71**, 2703.
18 J. Jeener, B. H. Meier, P. Bachman and R. R. Ernst, *J. Chem. Phys.*, 1979, **71**, 4546.
19 (*a*) Y. Machida, H. Nishi and K. Nakamura, *Chirality*, 1999, **11**, 173; (*b*) D. Gehin, P. A. Kollman and G. Wipff, *J. Am. Chem. Soc.*, 1989, **111**, 3011.
20 R. Freeman and H. D. W. Hill, *J. Chem. Phys.*, 1969, **51**, 3140.
21 D. Marion and K. Wuthrich, *Biochem. Biophys. Res. Commun.*, 1983, **113**, 967.
22 A. Bax and D. G. Davis, *J. Magn. Reson.*, 1985, **63**, 207.
23 A. Bax and M. F. Summers, *J. Am. Chem. Soc.*, 1986, **108**, 2093.
24 Z. Li and H. A. Scheraga, *Proc. Natl. Acad. Sci. USA*, 1987, **84**, 6611.
25 I. Kolossvary and W. C. Guida, *J. Comput. Chem.*, 1993, **140**, 691.